

# Numerical Simulation for Quasi-Brittle Interface Fracture in Cementitious Bi-material System

Y.M.Lim, M.K.Kim & S.K.Shin

*Applied Mechanics Lab., Dept. of Civil Engineering, Yonsei University, Seoul (120-749), Korea*

V.C.Li

*ACE-MRL, Dept. of Civil Envir. Eng., Universit of Michigan, Ann Arbor, MI 48109, USA*

**ABSTRACT:** An interface appears whenever a repair material is applied to an infrastructure system for rehabilitation. Usually the interface is relatively weaker than the both side materials in a repair system such as a concrete overlay on bridge decks or pavements. So, there is high chance to fail along the interface in repaired systems because of the stress concentration and rapid change of stress level along the interface. Many attempts have been tried to characterize the interfacial behavior experimentally, whereas a limited number of numerical analysis based on fracture behavior has been performed. In this paper, numerical tool that can predict effectively the interfacial fracture behavior is developed using Axial Deformation Link Elements(ADLE) based on fracture energy concept. The simulated interface fracture behavior has the same trend with the experimental results in concrete/concrete repair system under mixed mode loading conditions. It is also shown that interface properties have much influence on the mechanical behavior of bi-material systems, and the predicted crack patterns are in good agreement with that observed experimentally under static loading conditions.

## 1. INTRODUCTION

Recently, the rehabilitations of concrete infrastructures are considered important problems not only in civil engineering community but also by general public(Allen,1993). Many concrete infrastructures have been rehabilitated to extend the service life or restore the original strength of structures. In the rehabilitated systems, the interface between the newly applied material and the old substrate always appears whenever a repair material applies to an old substrate(Warner,1984). This interface is usually recognized as the weakest part in the repaired systems. Also, the performance of repaired system is strongly dependent on the performance of interface in many cases. For example, the performance of the interface in an overlay on a bridge deck or a pavement is a critical point for the system performance(Calvo,1991). Thus, the improvement of mechanical behavior of interface is a key issue in rehabilitation of concrete infrastructures as well as the selection of a repair material.

Many studies have been focused on measuring the interfacial material properties that can characterize the failure behavior of the interface. Commonly, tensile and shear strength of an interface have been widely accepted in practice. However, the failure mechanism of an interface is normally related to

cracking on the interface or kink cracking out of the interface. Thus, the strength concept of bi-material at an interface is not applicable much as the strength of a monotonic solid is not valid when the failure is governed by fracture. Recently, interface fracture mechanics has been applied to characterize the failure behavior of an interface in cementitious materials. Interfacial fracture toughness has been measured as a function of the phase angle in concrete-concrete, and concrete-cementitious composite interface system. Also, these measured values have been utilized to predict when the interface crack kinks from the interface. However, this prediction is limited only to a brittle interface. Thus, it is difficult to predict the path of an interface crack for quasi-brittle interface in realistic problems.

In many cases, the prediction of the interface crack propagation is needed. So, the numerical simulation technique for cementitious bi-material systems is developed based on fracture mechanics concept. Interface, substrate and repair material are modeled using ADLE(Axial Deformation Link Element).

The developed method was verified to provide accurate simulation of fracture propagation in quasi-brittle mono-materials. Interface fracture toughness test specimens are also then numerically modeled using the same technique. The simulated interfacial fracture toughness and experimentally measured one

is compared in this study. Thus, the developed technique demonstrates the capability of prediction for the interface crack propagation as well as load-deflection relationship.

Interfacial fracture toughness concept based LEFM is limited only to judge a kink condition of a brittle interface crack. Additionally, the interface fracture behavior in an quasi-brittle interface system is not fully understood yet. Thus, the developed numerical simulation technique that can predict the crack propagation with load-deflection relations in a quasi-brittle interface might help to understand the quasi-brittle interfacial fracture behavior and can be utilized in many different aspects for interface failure mechanism in real problems.

## 2. AXIAL DEFORMATION LINK ELEMENT

### 2.1 Fictitious crack model

To model the interface fracture behavior, the fictitious crack model is introduced. The required material properties of an interface are elastic modulus  $E$ , tensile strength  $f_t$  of interface and fracture energy  $G_F$ . The constitutive relations, stress-crack separation relations, is determined using these material properties. The constitutive relation up to the tensile strength is characterized by the elastic modulus of the material. On the other hand, the post peak constitutive relation is characterized by the stress-separation  $\sigma(w)$  curve as shown in Figure 1.

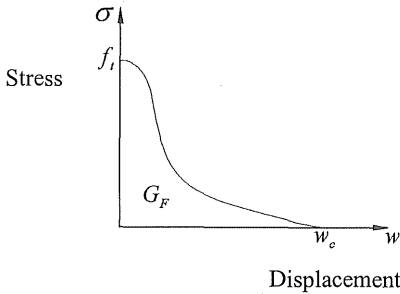


Figure 1. Fictitious crack model

The constitutive relation that is based on fictitious crack model developed by Hillerborg(1976) is adopted as a theory for numerical calculation of crack propagation in a quasi-brittle material. It is assumed that the area under stress-separation curve is constant and is considered as a material fracture parameter(fracture energy)  $G_F$  given as Equation 1

$$G_F = \int_0^{w_c} \sigma(w) dw \quad (1)$$

where,  $w_c$  is the critical crack separation at vanishing stress.

### 2.2 Constitutive relations

Tensile constitutive relations are based on the fictitious crack model, and the softening behavior of the interface is implemented through the stress-crack separation relations in order to arrive at a mesh-objective relation. The relationships between the stress( $\sigma$ )-separation( $w$ ) are assumed as Equation 2

$$\sigma = f_t(1 - w/w_c) \quad (2)$$

where,  $\sigma$ : stress at separation  $w$ ,  $f_t$ : tensile strength, and  $w_c$ : separation at vanishing stress given as Equation 3

$$w_c = \frac{2G_F}{f_t} \quad (3)$$

where,  $G_F$ : fracture energy of a quasi-brittle material. The stress at any given displacement can be calculated as Equation 4 and depicted in Figure 2

$$\sigma = Eu/l_e \quad \text{for } u \leq u_p \quad (4a)$$

$$\sigma = \sigma(u) \quad \text{for } u > u_p \quad (4b)$$

$$\sigma = 0.0 \quad \text{for } u > u_u \quad (4c)$$

where,  $u_p$ : displacement at elastic limit,  $u_u$ : displacement at ultimate state,  $l_e$ : element length, and  $\sigma(u)$  given as Equation 5 is a function to calculate stresses based on the proposed model(Gopalaratnam,1985).

$$\sigma(u) = f_t \exp(A(u - u_p)/(u_u - u_p)) \quad (5)$$

where, A is constant determined by fracture energy.

The initial stiffness matrix( $k_0$ ) is utilized to the stiffness degradation right after the peak load for each element. The re-constructed stiffness matrix( $k_m$ ) is calculated using previous solution according to the stiffness matrix  $k_{m-1}$ . The softening behavior of the failure mechanism is implemented through this iteration procedure.(Ashraf,1997)

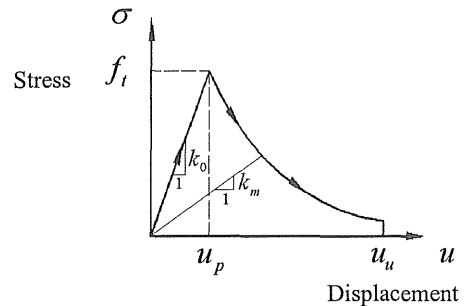


Figure 2. Constitutive relations

### 3. VERIFICATION OF ADLE ON MONO-MATERIAL

#### 3.1 Cracking behavior of direct tensile specimen

In this section, numerical analysis under direct tensile loading is performed to verify the developed numerical technique on ordinary quasi-brittle mono-material. The load is applied through displacement control at one end, while the other end is prevented from vertical and horizontal movements. Dimensions of the specimen are 2.54cm×2.54cm, and the test specimen and numerical modeling is specified in Figure 3.

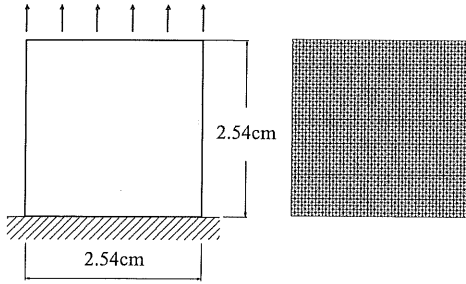


Figure 3. Test specimen and numerical modeling

The material properties used in these simulations are as follows : tensile strength 3.48MPa, elastic modulus 31.7GPa, and fracture energy 100N/m. The material properties for each element are assigned probabilistic. For the probabilistic approach, Monte Carlo simulation is performed using a normal distribution. The length of ADLE used in the modeling is 0.508mm each, and the number of the elements is 7600 with c.o.v 10%. The stress-strain curve of experimental and numerical results are illustrated in Figure 4. The shape of the predicted stress-strain curve including the peak load and softening branch is almost identical to those observed experimentally(Lee,1991). Figure 5 shows the procedure from crack initiation to crack propagation.

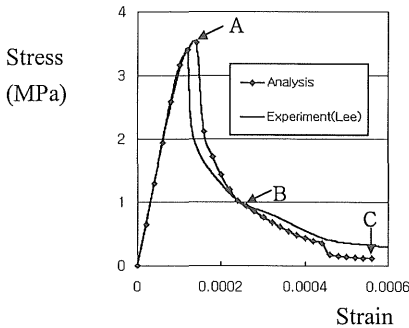


Figure 4. Stress-strain curve

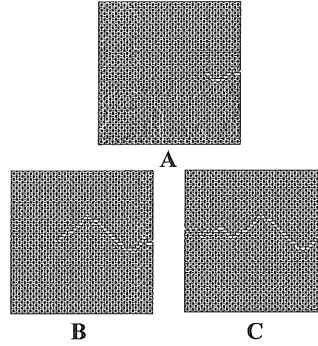


Figure 5. Crack propagation

#### 3.2 Cracking behavior of notched beam

Initial notched beam has also been simulated under 3-point flexural loading to verify the proposed model with stress concentration. The length and depth of the specimen are 19.5cm and 7.8cm respectively. The other dimensions and numerical modeling are specified in Figure 6. The used material properties are the same as those of experiment(Bazant,1983). Tensile strength is 2.97MPa and elastic modulus is 28.06GPa. The fracture energy is assumed as 145N/m in the range of ordinary concrete. In this case, the length of ADLE is 3.81mm, and the number of elements is 3062 with c.o.v 10%. Displacement control method is applied to investigate the softening behavior.

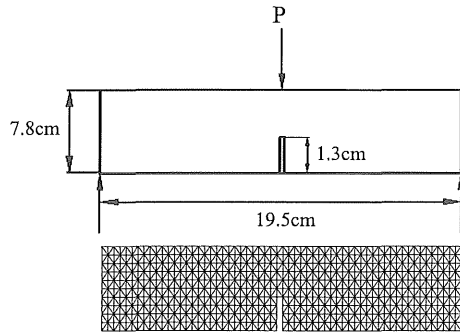


Figure 6. Test specimen and numerical modeling

The load-displacement curve of the experiment and numerical analysis are illustrated in Figure 7. In this figure, good agreement is obtained between the predicted and experimental data in the simulated range. The discrepancy of initial stiffness in the elastic range may be attributed to the difference of boundary conditions. The boundary conditions implemented in the simulations are ideal unlike those of experiment. The difference at the peak load is well matched. The discrepancy found in the softening region may come from the value of

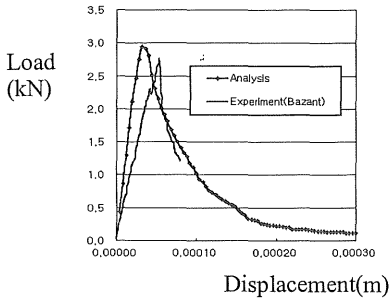


Figure 7. Stress-displacement curve

fracture energy which is not presented in the experiment. Agreement between numerical and experimental results in Figure 7 is expected to improve by using a more accurate value of fracture energy in the numerical simulation.

The behavior due to the ratio of  $a/w$  (notch depth/beam depth) is investigated. The load-displacement curve is illustrated in Figure 8, and crack propagation is depicted in Figure 9. The peak load decrease as the notch depth increase, and this behavior is identical to the predicted experimental result. Crack propagating behavior is also comparable with experimental results. Crack initiates due to the stress concentration at the notch tip, and propagates along the weak part of the nominal specimen to the loading point until the final failure occurs.

From the results of section 3.1, 3.2, it is shown that the proposed numerical technique can be used to model the failure behavior of quasi-brittle mono-material based on fracture mechanics.

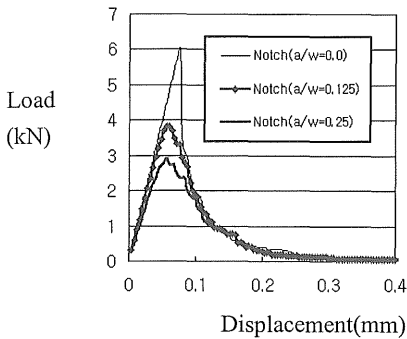


Figure 8. Load-displacement curve due to  $a/w$

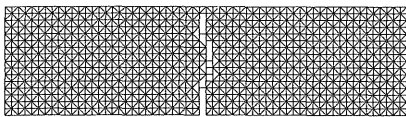


Figure 9. Crack propagation

## 4. VERIFICATION OF ADLE ON BI-MATERIAL

### 4.1 Outline of modeling

Numerical simulations are performed to investigate the applicability of the developed numerical technique to the bi-material system having interface. The length of the specimen is 45.72cm, and the other dimensions are specified in Figure 10. To prevent the flexural failure, a varied thickness specimen is developed in experimental program (Lim, 1997, 1998). In the experiment, specimen is strengthened by increasing the thickness at the maximum bending moment area to prevent from premature failure. In this numerical study, the tensile strength increases two times at the maximum bending moment area to have the same strengthening effect in experimental specimens. A bending specimen set-up with symmetric and asymmetric loading configurations is selected for the mixed loading condition (Lim, 1997, 1998), and its schematized view is shown in Figure 11. Where, A and B are 7.62cm, 12.54cm respectively. The symmetric set-up can provide interface fracture toughness at zero phase angle when there is no material mismatch.

As shown by the asymmetric set-up, the relative amounts of shear force and bending moment which create the shear and normal stress at the crack tip are changed with the varied "offset"  $s$ . Thus, various

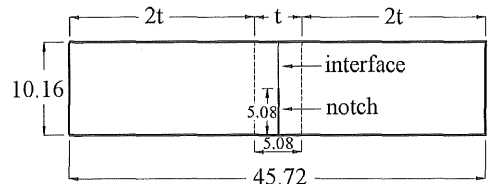


Figure 10. Dimension of specimen ( $t=3.81$ , unit:cm)

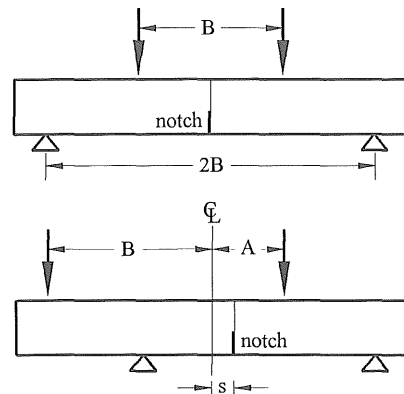


Figure 11. Set-ups and loading configurations

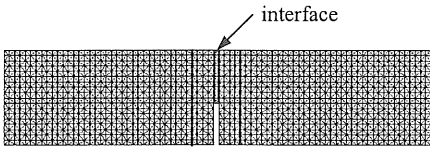


Figure 12. Numerical modeling

phase angles can be arranged from  $0^\circ$  to  $80^\circ$  using single specimen geometry.

To simulate the interface fracture toughness test, ADLE method based on the fracture energy concept is adopted. The numerical modeling of specimen is shown in Figure 12 and the material properties of each material are tabulated in Table 1. In this numerical technique, the fracture energy for interface is needed to specify only at phase angle  $0^\circ$ . This can simulate the varied interfacial fracture energy along phase angle. The interfacial material properties ( $f_t$ ,  $E$  and fracture energy at phase angle  $0^\circ$ ) are determined from parametric study of interface fracture.

Table 1. Material properties used in numerical simulation

Material	Young's modulus, $E$ (GPa)	Tensile strength, $f_t$ (MPa)	Fracture energy, $G_F$ (N/m)
Base material	25.8	3.5	90
Repair material	24.9	3.5	90
Interface	10.0	2.8	30

#### 4.2 Experimental and numerical results

In a concrete/concrete interface system, numerical and experimental results (Lim, 1997, 1998) on interface fracture toughness with varied phase angle ranging from  $0^\circ$  to  $80^\circ$  is illustrated in Figure 13. The numerical results were illustrated by two curves with the mesh size of 1563 elements (element length 0.00576mm) and 10880 elements (element length 0.0036mm). From the analysis, it has been found that the numerical result becomes almost independent of the mesh size. In the experimental data, upper and lower bound values are presented at phase angle  $0^\circ$ ,  $30^\circ$ ,  $60^\circ$  and  $75^\circ$ . Both numerical and experimental results increase as the phase angle increases. The numerical results have a good agreement with the experimental results.

The experimental failure mode is illustrated in Figure 14 at phase angle  $60^\circ$ , and the numerical results at each phase angle are illustrated in Figure 15(a-c). Three different failure modes are found in

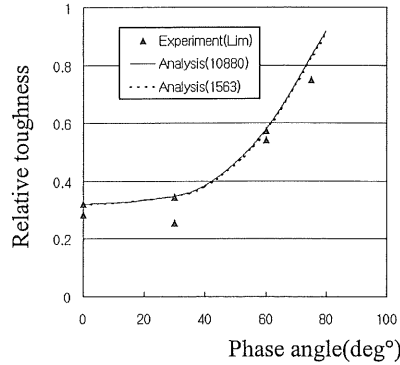


Figure 13. Interface fracture toughness

these interface fracture toughness results. In the first, the interface crack clearly propagates along the interface in the case of the phase angle  $0^\circ$  (see Figure 15a). In the second mode, the interface crack propagates along the interface in the beginning and

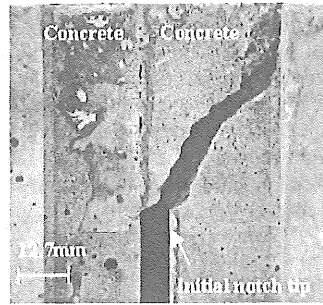


Figure 14. Interface cracking and kinking behavior in concrete/concrete system (Lim, 1997, 1998) (phase angle about  $60^\circ$ )

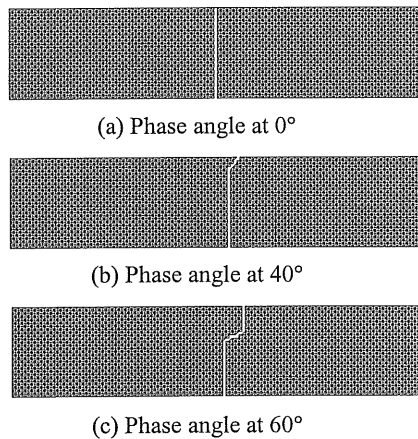


Figure 15. Failure modes for each phase angles

then it kinks from the interface in the case of the phase angle  $40^\circ$ (see Figure 15b). In the third mode, the interface crack kinks out from the interface(see Figure 15c). This failure mode is comparable to the experimental results, and the failure mode for phase angle  $60^\circ$  is illustrated in Figure 14. These results can be explained by the kinking condition of interface crack propagation, which is shown in Figure 16.

## 5. FAILURE BEHAVIOR DUE TO INTERFACE PROPERTIES

### 5.1 Behavior due to interface toughness( $G_c$ )

In this study, the mechanical behavior of the concrete/concrete specimen under 4-point loading conditions is characterized due to the fracture toughness  $G_c$ . The phase angles are ranged from  $0^\circ$  to  $80^\circ$ , and the fracture toughness of the interface is 12N/m, 17N/m and 23N/m respectively. Response between the relative driving force and relative interface toughness due to the phase angle is illustrated in Figure 16. When the relative driving force is greater than the relative interface toughness, an interface crack will kink out from the interface. The relative toughness increase as the interface toughness is higher at the same phase angle, and this result is identical to the response observed in the real situation. As shown in the Figure 17, kinking condition is not satisfied at points A and B, because relative driving force is greater than the relative toughness. Thus, crack propagates along the interface at the beginning, and then kinks out from the point where stress change. In the case of C and D points, the crack kinks out from the interface directly because the kinking condition is satisfied. However, it can be seen that crack at point C propagates slightly along the interface and kinks out. This phenomenon is also observed in the experiment(see Figure 14), and it may be associated

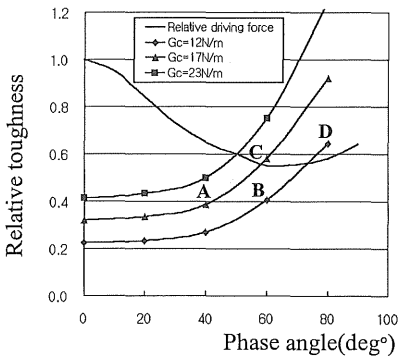


Figure 16. Relative driving force and relative toughness

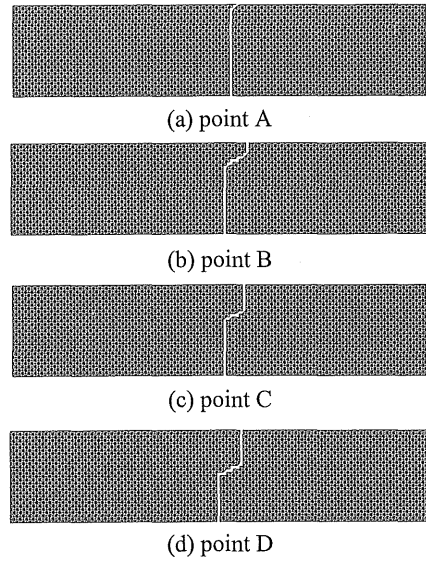
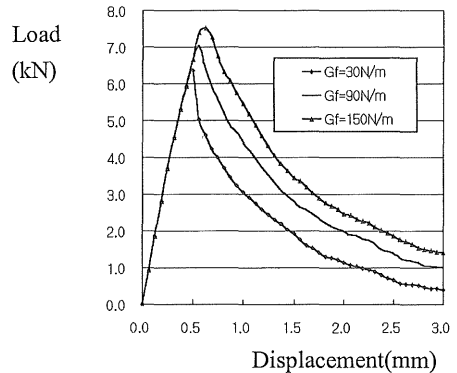
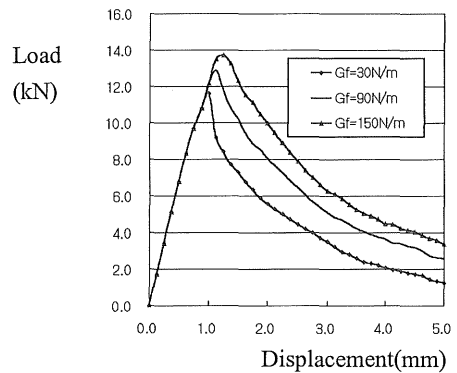


Figure 17. Failure modes at each point



(a) Phase angle  $40^\circ$



(b) Phase angle  $80^\circ$

Figure 18. Load-displacement curve due to fracture energy

with the shape of the notch tip. In the case of numerical analysis, it may come from the probabilistic distribution of material property.

### 5.2 Behavior due to interface fracture energy( $G_F$ )

The variation of fracture energy  $G_F$  used in this simulation is 30N/m, 90N/m and 150N/m. Load-displacement response due to fracture energy at phase angle  $40^\circ$ ,  $80^\circ$  is illustrated in Figure 18. As the fracture energy of the interface increases, the peak load of the response increases and the area of the softening region becomes larger. The load-displacement curves have the same shape at different phase angles.

The interface toughness vs. phase angle response is shown in Figure 19. In this figure, the variation of interface toughness due to the change of  $G_F$  value is not significant. However, softening branch vary with each other due to the  $G_F$  at right after the

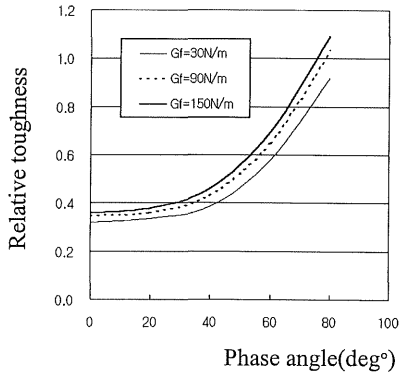


Figure 19. Interface toughness due to fracture energy

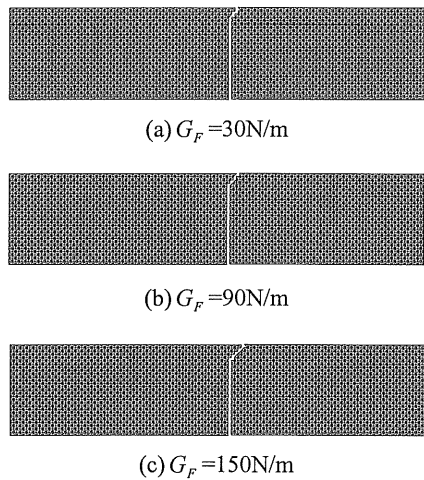


Figure 20. Crack behavior at phase angle  $40^\circ$

peak. When the  $G_F$  is smaller, the steeper drop of softening branch can be observed(see Figure 18). The crack propagation due to the interfacial fracture energy at phase angle  $40^\circ$  is illustrated in Figure 20. The kinking angle change also noticed with variable  $G_F$  when the interface crack kinks out(see Figure 20), and the research on this result have to be carefully investigated in further studies.

The interface properties such as fracture toughness and fracture energy have influence on the mechanical behavior of bi-material systems. However, the influence according to the fracture energy is not sensitive as that of fracture toughness in this study.

## 6. CONCLUSIONS

In this paper, a numerical tool that can predict effectively the interfacial fracture behavior is developed using ADLE based on fracture energy concept. The developed numerical technique can accurately predict the complete mechanical response of quasi-brittle mono-materials, including softening, under different static loading conditions. Also, it is shown that the interface fracture behavior can be analyzed accurately using this developed numerical technique. The model predictions are in good agreement with the experimental results. Thus, this developed numerical technique can simulate the interface fracture behavior under different geometry and loading conditions.

It is also tentatively shown by the parameter study that interface toughness  $G_c$  have much influence on the interface fracture behavior of bi-material systems, and further studies is required on the effect of fracture energy  $G_F$ .

## ACKNOWLEDGEMENT

The authors acknowledge the financial support(grant number E00508) obtained from the Korea Research Foundation.

## REFERENCES

- Allen, R.T.L., Edwards, S.C. and Shaw, J.D.N. (1993) **Repair of Concrete Structures**, Chapman and Hall, London, UK.
- Warner, J. (1984) **Selecting Repair Material – Some Important Material Properties that Should be Considered**. Concrete Construction.
- Calvo, L. and Meyers, M. (1991) **Overlay Materials for Bridge Deck**. Concrete International, 13(7), 46-47.
- Hillerborg, A. Modeer, M. and Petersson, P.E. (1976) Analysis of Crack Formation and Crack Growth in Concrete by means of Fracture Mechanics and Finite Elements, **Cement and Concrete Research**, 6, 773-782.

Gopalaratnam, V.S. and Shah, S.P. (1985) Softening Response of Plain Concrete in Direct Tension, **ACI Journal**, Technical Paper, 310-323.

Ashraf, R.A.M. (1997) **Micromechanics of Concrete Behavior and Progressive Failure under Static Loading**, Ph.D. Thesis, University of Michigan, Ann Arbor.

Lee, J.H. (1996) **Theory and Implementation of Plastic-Damage Model for Concrete Structures under Cyclic and Dynamic Loading**, Ph.D. Thesis, University of California, Berkeley.

Bazant. Z.P. (1983) **Crack Band Theory for Fracture of Concrete**. RILEM Materials and Structures, 16, 155-177.

Lim, Y.M. and Li, V.C. (1997) Durable Repair of Aged Infrastructures Using Trapping Mechanism of Engineered Cementitious Composites, **Cement and Concrete Composites**, 19(4), 373-385.

Lim, Y.M. and Li, V.C. (1998) Characterization of Interface Fracture Behavior in Repaired Concrete Infrastructures, in **Proceedings FRAMCOS-3**, Gifu, Japan, 2, 1817-1828.

Li, V.C., Horii, H., Kabele, P., Kanda, T. and Lim, Y.M. (2000) Repair and Retrofit with Engineered Cementitious Composites, **Engineering Fracture Mechanics**, 65(2-3), 317-334.

Lim, Y.M., Kim, M.K, Shin, S.K. and Heo, W.Y. (1999) Numerical Simulation for the Interface Behavior between the Substrate and Repair Material Based on Fracture Energy Concept. in **Proceedings APCOM '99**, Singapore, Dec., 1, 341-346.

Elfgren, Z. (1989) **Fracture Mechanics of Concrete Structures** (Report of RILEM Tech. Committee TC 90-FMA), Chapman and Hall, London, UK.

Ulfkjaer, J.P., Krenk, S. and Brincker, R. (1992) Analytical Model for Fictitious Crack Propagation in Concrete Beams. **Journal of Engineering Mechanics**, 121, 7-15.

Gopalaratnam, V.S. and Shah, S.P. (1985) Softening Response of Plain Concrete in Direct Tension. **ACI Journal**, 310-323.